IOPscience iopscience.iop.org

Home Search Collections Journals About Contact us My IOPscience

Scanning tunneling microscopy study of higher-order Si(100)-c(8 × 8) surface reconstruction

This article has been downloaded from IOPscience. Please scroll down to see the full text article.

2008 J. Phys.: Condens. Matter 20 395003

(http://iopscience.iop.org/0953-8984/20/39/395003)

View the table of contents for this issue, or go to the journal homepage for more

Download details:
IP Address: 129.252.86.83
The article was downloaded on 29/05/2010 at 15:10

Please note that terms and conditions apply.

J. Phys.: Condens. Matter **20** (2008) 395003 (6pp) doi:10.1088/0953-8984/20/39/395003

Scanning tunneling microscopy study of higher-order Si(100)-c(8 × 8) surface reconstruction

M A K Zilani[1,2], H Xu[1], X-S Wang[1], Nikolai Yakovlev[3] and A T S Wee[1,4]

[1] Department of Physics, 2 Science Drive 3, National University of Singapore, Singapore 117542, Republic of Singapore
[2] Department of Physics, Rajshahi University of Engineering and Technology, Rajshahi 6204, Bangladesh
[3] Institute of Materials Research and Engineering (IMRE), 3 Research Link, Singapore 117602, Republic of Singapore

E-mail: phyweets@nus.edu.sg

Received 3 March 2008, in final form 25 July 2008
Published 19 August 2008
Online at stacks.iop.org/JPhysCM/20/395003

Abstract
We have studied the higher-order Si(100)-c(8 × 8) surface reconstruction using scanning tunneling microscopy (STM) and low-energy electron diffraction (LEED). Our high resolution STM images show that long range ordering of *rectangular cells* are the building blocks of this reconstruction. We identify Si–Si ad-dimers and determine that three pairs of ad-dimers constitute each rectangular cell. The ad-dimer direction is parallel to the longer side of these rectangular cells. We propose a new dimer model to explain this reconstruction.

(Some figures in this article are in colour only in the electronic version)

1. Introduction

Si(100) is a widely studied surface due to its importance both in the semiconductor industry and the scientific community. The most commonly observed reconstruction on clean Si(100) is the (2 × 1) formed by dimerization of the top-layer atoms [1]. Since this reconstruction was first observed almost half a century ago by LEED, it has been studied extensively by both theory and experiment [2]. Defects, impurities and surface cleaning procedures play a vital role in the formation of other reconstructions observed on this surface. The second most-studied reconstruction on this surface is the (2 × n) (where $6 < n < 11$), formed by missing dimer channels along the Si dimerization direction [3]. Though there are reports that suggest that this reconstruction may form on clean Si(100) quenched from high temperatures, it is widely accepted that trace amounts of metal impurities, particularly Ni, on the surface are responsible for this reconstruction [4, 5].

Theoretical studies based on tight binding energy minimization calculations have proposed that the ground-state reconstruction should be either p(2 × 2) or c(4 × 2) rather than (2 × 1) [6]. A number of recent experimental studies have addressed the (4 × 2) reconstruction and its phase transition from the (2 × 1) (or p(2 × 2)) reconstruction [7–10]. The p(2 × 2) and c(4 × 2) phases that consist of buckled dimers, which is the ground-state configuration, is still not fully resolved [9–13]. In the last two decades, STM has played a powerful role in the study of surface reconstructions on metal and semiconductor surfaces. Higher-order reconstructions have been predicted by theoretical studies and occasionally observed by LEED, STM and electron energy-loss spectroscopy (EELS) [5, 14–17]. These higher-order reconstructions have a higher surface energy than Si(100)-(2 × 1) and consist of periodic arrangements of defects (missing dimers) and ad-dimers. The higher-order c(4 × 4) on Si(100) was first predicted by Pandey based on total-energy calculations and later observed experimentally by LEED and STM [14, 16, 18, 19]. Based on a first-principles pseudopotential method and local density approximation, Uhrberg *et al* calculated the total energy and electronic structure for three different models of the c(4 × 4) reconstruction and compared the energy with the (2 × 1) buckled dimer structure [18]. As a high surface energy results

[4] Author to whom any correspondence should be addressed.

 © 2008 IOP Publishing Ltd Printed in the UK

in poor stability, only a few higher-order reconstructions have been directly observed by STM.

The higher-order Si(100)-c(8 × 8) reconstruction has been observed and studied by LEED, EELS and STM [5, 15, 17]. There is only one STM study that directly observes and explains this c(8 × 8) reconstruction [15]. Another recent STM study observed a similar surface topography with c(4 × 8) reconstruction [20]. *Rectangular cells* are the building blocks of these reconstructions. In the report by Murray *et al*, the STM image shows that the rectangular cells of the c(8 × 8) reconstruction do not cover the whole surface, and there are areas where the (2 × *n*) is clearly visible [15]. Using STM and LEED, we observed a stable c(8 × 8) reconstruction that extended over the whole surface. Neither the (2 × *n*) nor any other reconstruction was visible. With our high resolution STM images, we clearly identify the ad-dimer direction on the surface, which is parallel to the longer side of the rectangular cells. A new dimer model is proposed where three pairs of ad-dimers form in each rectangular cell.

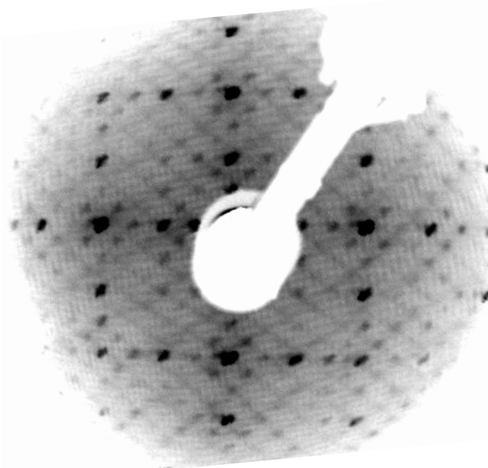

Figure 1. Low-energy electron diffraction pattern recorded from Si(100) at 95 eV showing c(8 × 8) periodicity. This image has been presented in inverted contrast to make the spots clearer.

2. Experimental details

In situ experiments were performed in a multi-chamber ultra-high vacuum (UHV) system with a base pressure of 2×10^{-10} mbar [21]. The analysis chamber is equipped with an Omicron VT-STM, x-ray photoelectron spectroscopy (XPS) and LEED. We used boron-doped p-type Si(100) substrates ($\rho = \sim 10\ \Omega$ cm) manufactured by Unisil Corporation, USA for our experiments. We used direct current resistive heating Omicron sample holders to anneal the Si samples (8×2 mm^2). The c(8 × 8) reconstruction was observed after degassing the sample at 650 °C for 10 h, flashing to 1200 °C, followed by fast cooling to 700 °C, maintaining at this temperature for 5 min, and finally slow cooling over a period of 10 min to room temperature (RT). We repeated the flash cycles (10–12 times), keeping the sample at 1200 °C for a few seconds while maintaining the chamber pressure below 1×10^{-9} mbar. Direct current was used for annealing the samples and ∼5.5 A current (with ∼4.2 V biasing voltage) was applied to achieve a flashing temperature of about 1200 °C. The substrate temperature above 600 °C was measured with an optical infrared pyrometer. We have confirmed these temperature readings by calibrating the values of direct current passed through the sample. The sample temperatures were measured with an estimated accuracy of ±25 °C. Usually the terraces were of single-layer height; however, at a few places on the surface we have also observed step bunching involving two or three layers. XPS and time-of-flight secondary ion mass spectroscopy (ToF-SIMS) were employed to analyze the surface contamination. The Si(100) samples studied were found to be clean, with contaminant levels below XPS detection limits of <1 at.%. ToF-SIMS (ION-TOF) was employed to detect trace levels of contaminants below the XPS detection limit.

3. Results

Figure 1 is a LEED pattern taken at 95 eV, which shows c(8 × 8) periodicity. This pattern was consistent at different positions of the sample surface and comparable with previously published LEED results of Si(100)-c(8 × 8) [5, 15, 17]. In previous STM observations, the c(4 × 8) and c(8 × 8) reconstructions always appeared intermixed with the (2 × *n*) phase [15, 20]. However, in our present work we did not observe any other surface reconstruction coexisting with c(8 × 8). Zhao *et al* obtained the c(4 × 8) reconstruction by the following procedure: Si deposition on Si(100)-2 × 1 using molecular beam epitaxy followed by annealing, resulting in the Si(100)-2 × *n*, and finally 2 ML additional Si deposition yielding the c(4 × 8) reconstruction [20]. Murray *et al* obtained the c(8 × 8) reconstruction by a conventional cleaning procedure that normally produces the Si(100)-2 × 1 reconstruction, but found very low Cu traces by SIMS, in which Cu density is below the detectable limit of conventional Auger electron spectroscopy [15]. On our as-prepared c(8 × 8) surface, XPS showed no surface contamination up to its detection limit of 1%. In order to obtain more sensitive data about possible surface contamination, we analyzed the surface using ToF-SIMS. The ToF-SIMS system has the advantage of high mass resolution, parallel detection of all masses and unlimited mass range. This allows operation in the regime of surface spectroscopy where a mass spectrum with a good signal-to-noise ratio can be obtained after sputtering less than one atomic layer. We quickly transferred the sample *ex situ* into a ToF-SIMS chamber with argon protection to alleviate ambient contamination. A comparison of the ToF-SIMS results of the substrate showing the c(8 × 8) reconstruction with another Si(100) sample cleaned *ex situ* using hydrogen fluoride solution reveals trace amounts of Cu and Mg on the former.

The problem of Cu incorporation during wafer polishing has been reported in several studies [22]. It is believed that, in boron-doped Si samples, Cu forms a boron–copper complex in Si wafers [23, 24]. Reports suggest these boron–copper complexes are metastable even at room temperature; they dissociate and allow Cu to assume interstitial positions. Cu is a rapid diffuser in Si [25] and, during low temperature annealing, interstitial copper diffuses to the surface of the

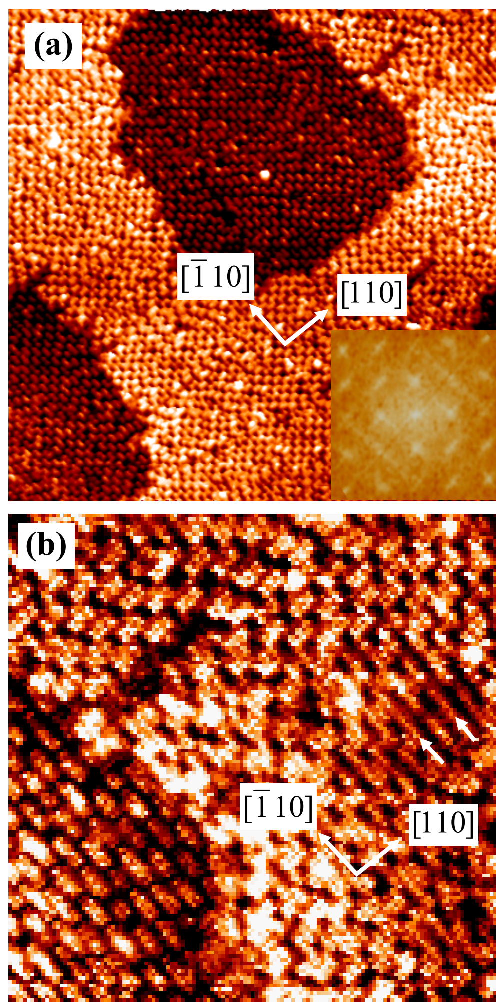

Figure 2. Empty-state STM image of the Si(100)-c(8 × 8) reconstruction taken at 2.0 V and 0.16 nA. (a) Scan size 1200 Å × 1200 Å showing long range ordering of the reconstruction. Inset shows the FFT representation of this STM image. (b) Scan size 400 Å × 400 Å (a close-up view of the upper right corner of the above image) showing a portion of the surface with irregular arrangement of rectangular cells where we can identify single long dimer rows, shown by arrows.

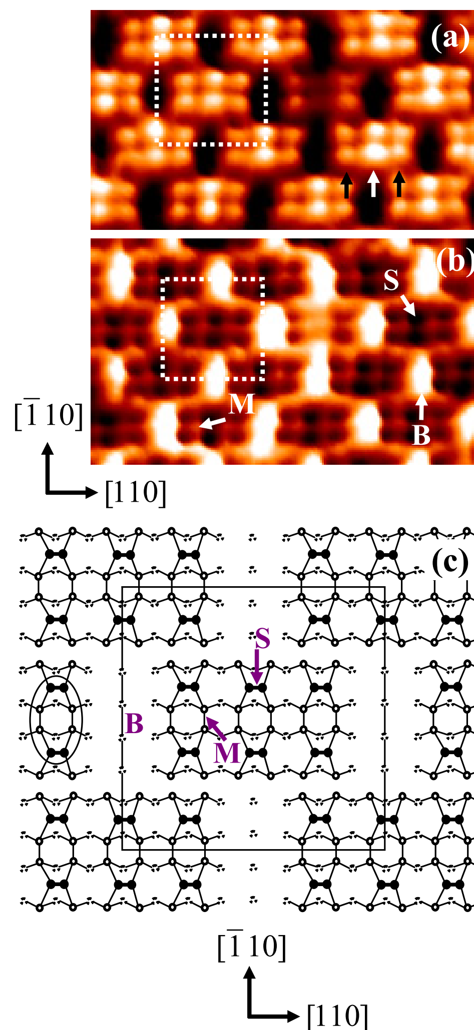

Figure 3. (a) Empty-state STM image (scan size = 108 Å × 62 Å, V = 2.0 V) of a small region of the Si(100)-c(8 × 8) reconstructed surface. Here the [110] direction is along the longer direction of the rectangular cells. A single Si(100)-c(8 × 8) unit cell is identified by the dotted square. (b) The same region with inverted contrast. The deepest portion of the surface topograph appears here as brightest (highest). Bottom, middle and surface layers are marked by B, M and S, respectively. (c) Proposed model to explain the Si(100)-c(8 × 8) reconstruction. The first, second and third layer of atoms are denoted by solid, hollow and dotted circles, respectively. For simplicity, dimerization of third-layer Si atoms (within the *rectangular holes*) is not considered here.

wafer [26]. Here, we believe that maintaining the substrate at 700 °C for 5 min and then slow cooling to RT enhances the surface Cu contamination. We confirmed the presence of trace amounts of Cu and Mg on the reconstructed surface by SIMS measurements. We suggest these trace amounts of metal contamination contribute to the observed higher-order reconstruction. Jemander *et al* have previously reported that only 0.07 ML C is sufficient to obtain full coverage by the higher-order c(4 × 4) reconstruction [27].

Figure 2(a) is a 1200 Å × 1200 Å STM image of the surface showing rectangular repeat patterns covering the whole area. Scanning different positions of the surface gave similar images to that in figure 2(a). We have recorded the fast Fourier transform (FFT) of the STM image in figure 2(a) and presented it as an inset. As expected, there is a good agreement between the LEED pattern in figure 1 and the FFT representation of the STM image, suggesting long range ordering of the superlattice structure [28]. A close-up view of the upper right corner of figure 2(a), where some rectangular patterns are not regular, is presented in figure 2(b).

A small area (108 Å × 62Å) of the surface with the superlattice structure is presented in figure 3(a). An unit cell marked in figure 3(a), which we identify as c(8 × 8), is described in the following paragraphs. It is evident that each *rectangular cell* consists of three pairs of protrusions. The electronic height of the *middle pair* that appear as a pair of bright dots in the STM image (indicated by a white arrow in figure 3(a)) is higher than the two *end pairs* (indicated by black arrows). The *end pair* along the longer side of a

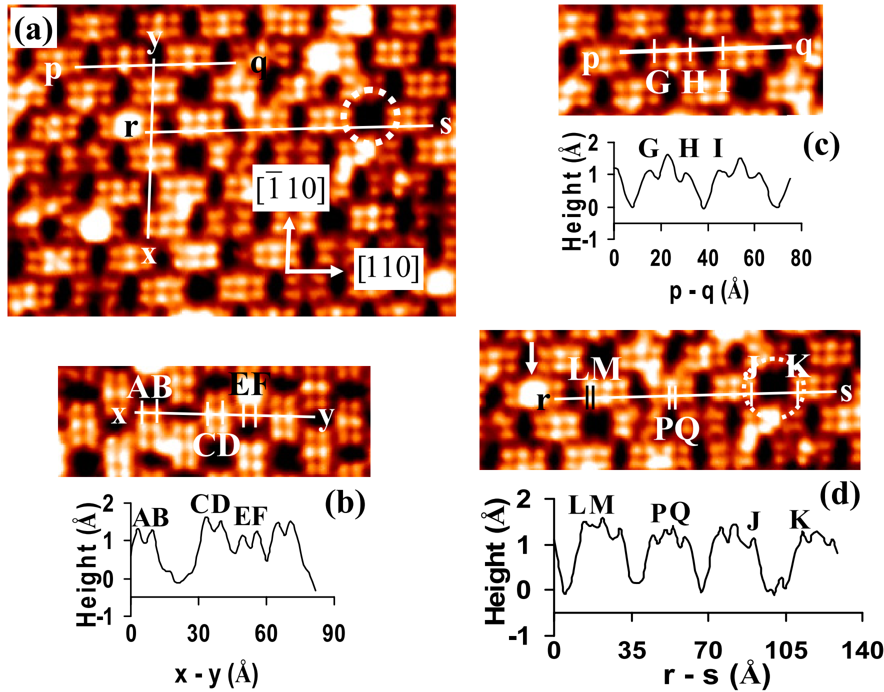

Figure 4. Line profiles *x*–*y* (along the [$\bar{1}$10] direction), *p*–*q* and *r*–*s* (both along the [110] direction) marked on the STM image (a) and presented separately in (b)–(d), respectively. The dotted circle in (a) shows a rectangular hole larger than normal. (c) shows three peaks within each *rectangular cell*, and that the electronic height of the *middle pair* is higher compared to the *end pairs*. LM and PQ in (d) show that each peak comprises of two components. The arrow in (d) identifies a particular *rectangular cell* with four pairs of ad-dimers.

rectangular cell is separated from the nearest *end pair* of the next *rectangular cell* by rectangular gaps of 15.6 ± 0.2 Å, corresponding to the length of one rectangular cell, forming a rectangular checkerboard repeat pattern. The [110] direction is along the longer side of the rectangular cells and is marked accordingly in figure 3.

Next we determine the line profiles *x*–*y* (along the [$\bar{1}$10] direction), and *p*–*q* and *r*–*s* (along the [110] direction), as marked on the STM image in figure 4(a). We present these line profiles separately in figures 4(b)–(d), respectively. The distance between the *end pair* A–B (as marked on line profile *x*–*y*, figure 4(b)) and C–D at the *middle pair* was found to be ~6.1 ± 0.2 Å. We measured the separation D–E between two neighboring pairs as ~9.5 ± 0.2 Å. Hence the total distance from C to E is ~15.6 ± 0.2 Å. The distance B–D we measured to be ~30.4 ± 0.2 Å. The values of C–E and B–D are very close to 4 × *a* (15.36 Å) and 8 × *a* (30.72 Å), respectively, where *a* is the primitive unit cell lattice parameter (~3.84 Å) of the unreconstructed Si(100) surface.

The line profile *p*–*q* (cf figure 4(c)) shows three peaks within each *rectangular cell*. Both the distances G–H and H–I (marked in figure 4(c)) we measured to be ~15.6 ± 0.2 Å, close to 4 × *a* (15.36 Å). Occasionally we observe a larger*rectangular hole* compared to other *rectangular holes*, possibly defect-related, as shown by the dotted circle in figure 4(a). The line profile *r*–*s* presented in figure 4(d) gives JK ~ 23.5 ± 0.2 Å, close to 6 × *a* (23.04 Å). In some areas on the STM images along the [110] direction (on the line profile *r*–*s*), we can resolve each peak into two smaller peaks, as can be seen at L–M and P–Q (figure 4(d)). The separation of both L–M and P–Q (cf figure 4(d)) is ~3.3 ± 0.2 Å. As this value is $<a$, it is postulated that this represents a single surface dimer.

It is evident from the line profile *r*–*s* (cf figure 4(d)) that the difference between highest and lowest points on the surface is ~1.7 ± 0.1 Å. The STM-measured electronic height may depend both on the finite tip size and bias voltage. The single-step height on Si(100) is ~1.4 Å [29], suggesting more than one layer is involved and we propose a new model of the Si(100)-c(8 × 8) reconstruction which is two layers deep (cf figure 3(c)). Here it should be mentioned that density functional theory calculations have not yet been done to simulate the STM images, and our model is based on a simple geometrical model. The dimensions of the model match the line profiles obtained from figure 4. The first, second and third layer atoms are denoted by solid, hollow and dotted circles, respectively. Here we only consider dimerization of Si adatoms at the top two layers, as shown in the model. The c(8 × 8) unit cell is identified by the square shown in the figure. To reduce the number of dangling bonds it is expected that the third layer atoms within the *rectangular holes* also form dimers (not shown here). The larger *rectangular hole* structure marked by the dotted circle in figures 4(a) and (d) can also be simulated in this model as a pair of local missing dimer defects.

To highlight the c(8 × 8) symmetry, an inverted image of figure 3(a) is presented in figure 3(b). The deepest portions of the surface topography appear here as the brightest spots and clearly show three layers. The bottom, middle and surface layers are marked as B, M and S, respectively (cf figures 3(b) and (c)). Our proposed model (cf figure 3(c)) is in accordance with these layers.

4. Discussion

Identifying the dimers was the key to understanding this reconstruction. In an earlier STM observation, Murray *et al* explained the c(8 × 8) reconstruction by postulating five consecutive dimers (with dimer direction orthogonal to the longer sides of *rectangular cells*) in a row to match the length of the rectangular pattern [15]. However, this model is not consistent with the three pairs of well-resolved spots in our high resolution STM image (cf figure 3(a)). Furthermore, the dimers in their model appear to have an Si–Si atom separation of about 5.3 Å (measured from the STM image), which is larger than a. They speculated that this larger separation is due to the lateral spread of the wavefunctions. In another report, Zhao *et al* observed and interpreted the STM image of the c(4 × 8) reconstruction [20]. They postulated three dimers each separated by $2 \times a$ along the longer side of the *rectangular cell* and proposed a corresponding model. However, along the $[\bar{1}10]$ direction, the distance between a pair of spots (A–B and C–D as marked in figure 4(b)) is ∼6.1 ± 0.2 Å by STM measurements. This distance is obviously larger than a single dimer.

We have identified each individual rectangular spot along the [110] direction in figure 3(a) as a single dimer. The line profile represented in figure 4(d) supports this and unambiguously identifies the orientation of the dimers. Our observation from figure 4(b) is C–D ∼ 6.1 ± 0.2 Å and D–E ∼ 9.5 ± 0.2 Å, with total C–E ∼ 15.6 ± 0.2 Å, which is very nearly equal to $4 \times a$. We postulate that, due to dimerization of second-layer atoms within the *rectangular cell* along the $[\bar{1}10]$ direction, a pair of top-layer ad-dimers (marked by an oval on the proposed model in figure 3(c)) appears closer (∼6.1 Å < 7.68 Å, i.e. less than $2a$) in STM images. We conclude that a *rectangular cell* consists of three pairs of dimers. The *middle pair* of dimers appears higher in STM images (compared to two *end pairs*) probably due to their different atomic (and hence electronic) environment.

It was suggested in previous studies [30] that the formation of the c(4 × 4) reconstruction is due to stress fields induced by small amounts of impurities such as bismuth or carbon in the sub-surface. Similar to c(4 × 4) [30, 31] we suggest that this c(8 × 8) reconstruction is also strain-induced, and surface stress provided by metal impurities probably plays a key role in its formation. The presence of the M layer in the inverted STM image (cf figure 3(b)) clearly suggests the protrusions of the *middle* and *end pairs* are well separated and the dimerization direction is not along the $[\bar{1}10]$ direction, as proposed by previous reports [15, 20]. Our identification of the dimer is further supported by figure 2(b) where, at several places, the *rectangular cells* of the c(8×8) reconstruction is not regular. From figure 2(b) one can clearly identify a long single dimer row that runs along the upper terrace (marked by arrows, along the $[\bar{1}10]$ direction). These rows run orthogonal to the rectangular cells, supporting our model of dimers aligning along the rectangular cells. No such rows were identified along the [110] direction. The appearance of a single Si–Si dimer row on Si(100) is a common phenomena and was observed in earlier STM studies [31, 32].

It should be mentioned that Liu *et al* [33] observed the c(8 × 8) reconstruction after direct deposition of Cu on Si(100). Their experimental results show a linear increase of bright features (i.e. *rectangular cells*) on Si(100)-(2 × 1) with increasing Cu coverage. According to their calculation and experimental observations, if the surface is completely covered by the perfect c(8 × 8) structure, it should contain 0.1875 ML Cu. They have proposed an atomic model with 12 Cu atoms at the topmost layer of each unit cell. Although we proposed different structural models, their work suggests that Cu is a likely contaminant that promotes the c(8 × 8) reconstruction. Note that we did not have a Cu source in our UHV chamber, and we suspect that the Cu coverage in Liu *et al*'s paper is much lower than reported.

5. Conclusion

We report a higher-order Si(100)-c(8 × 8) surface reconstruction using LEED and STM. High resolution STM images show long range ordering of the c(8 × 8) reconstruction over a wide area of the surface and three pairs of ad-dimers constituting a *rectangular cell*. ToF-SIMS results detected trace amounts of Cu and Mg on the sample surface. We identified the Si–Si ad-dimers and their arrangements within each *rectangular cell*, which are the building blocks of this particular reconstruction. A new dimer model is proposed to explain our STM results.

References

[1] Chadi D J 1987 *Phys. Rev. Lett.* **59** 1691
[2] Schlier R E and Farnsworth H E 1959 *J. Chem. Phys.* **30** 917
[3] Niehus H, Kohler U K, Coepl M and Demuth J M 1988 *J. Microsc.* **152** 735
[4] Kato K, Ide T, Miura S, Tamura A and Ichinokawa T 1988 *Surf. Sci.* **194** L87
[5] Muller K, Lang E, Hammer L, Grim W, Heilman P and Heinz K 1984 *Determination of Surface Structure by LEED* ed P M Marcus and F Jona (New York: Plenum) p 483
[6] Ihm J, Lee D H and Joannopoulous J J X J D 1983 *Phys. Rev. Lett.* **51** 1872
[7] Tabata T, Aruga T and Murata Y 1987 *Surf. Sci.* **179** L63
[8] Matsumoto M, Fukutani K and Okano T 2003 *Phys. Rev. Lett.* **90** 106103
[9] Yokoyama T and Takayanagi K 2000 *Phys. Rev.* B **61** R5078
[10] Hata K, Yoshida S and Shigekawa H 2002 *Phys. Rev. Lett.* **89** 286104
[11] Ramstad A, Brocks G and Kelly P J 1995 *Phys. Rev.* B **51** 14504
[12] Inoue K, Morikawa Y, Terakura K and Nakayama M 1994 *Phys. Rev.* B **49** 14774
[13] Northrup J E 1993 *Phys. Rev.* B **47** 10032
[14] Pandey K C 1985 *Proc. 7th Int. Conf. on the Physics of Semiconductors* ed D J Chadi and W A Harrison (New York: Springer) p 55
[15] Murray P W, Lindsay R, Leibsle F M, Wincott P L and Thornton G 1996 *Phys. Rev.* B **54** 13468
[16] Ide T and Mizutani T 1992 *Phys. Rev.* B **45** 1447
[17] Kubo T, Aruga T, Takagi N and Nishijima M 1997 *Japan. J. Appl. Phys.* **36** L975
[18] Uhrberg R I G, Northrup J E, Biegelsen D K, Bringans R D and Swartz L-E 1992 *Phys. Rev.* B **46** 10251
[19] Simon L, Stoffel M, Sonnet P, Kubler L, Stauffer L, Selloni A, De Vita A, Car R, Pirri C, Garreau G, Aubel D and Bischoff J L 2001 *Phys. Rev.* B **64** 035306

[20] Zhao Y F, Yang H Q and Pang S J 2000 *Phys. Rev.* B **62** R7715
[21] Xu H, Li Y G, Wee A T S, Huan C H A and Tok E S 2002 *Surf. Sci.* **513** 249
[22] Falster R J, Leoni F, Bricchetti M and Corradi A 2000 Process for the removal of copper from polished boron doped silicon wafers *US Patent Specification* 6100167 http://www.patentstorm.us/patents/6100167/description.html (MEMC Electronic Materials)
[23] Prescha T and Weber J 1992 *Mater. Sci. Forum* **83–87** 167
[24] Mesli A and Heiser T 1992 *Mater. Sci. Forum* **83–87** 161
[25] Ohkubo Y, Matsumoto K and Nagai K 2005 *Japan. J. Appl. Phys.* **44** 3793
[26] Shabani M B, Yoshimi T and Abe H 1996 *J. Electrochem. Soc.* **143** 2025
[27] Jemander S T, Zhang H M, Uhrberg R I G and Hansson G V 2002 *Phys. Rev.* B **65** 115321
[28] Widmer R, Groning O, Ruffieux P and Groning P 2006 *Phil. Mag.* **86** 781
[29] Wilk G D, Wei Y, Edwards H and Wallace R M 1997 *Appl. Phys. Lett.* **70** 2288
[30] Norenberg H and Briggs G A D 1999 *Surf. Sci.* **430** 154
[31] Mo Y W, Kleiner J, Webb M B and Lagally M G 1991 *Phys. Rev. Lett.* **66** 1998
[32] Esser M, Zoethout E, Zandvliet H J W, Wormeester H and Poelsema B 2004 *Surf. Sci.* **552** 35
[33] Liu B Z, Katkov M V and Nogami J 2000 *Surf. Sci.* **453** 137